

RESEARCH

Open Access



# A risk score model based on TGF- $\beta$ pathway-related genes predicts survival, tumor microenvironment and immunotherapy for liver hepatocellular carcinoma

Jingsheng Liao<sup>1,2</sup>, Qi Liu<sup>1,2</sup>, Jingtang Chen<sup>1,2</sup>, Zhibin Lu<sup>1,2</sup>, Huiting Mo<sup>1,2</sup> and Jun Jia<sup>1,2\*</sup>

## Abstract

**Background:** Transforming growth factor-beta (TGF- $\beta$ ) signal is an important pathway involved in all stages of liver hepatocellular carcinoma (LIHC) initiation and progression. Therefore, targeting TGF- $\beta$  pathway may be a potential therapeutic strategy for LIHC. Prediction of patients' tumor cells response requires effective biomarkers.

**Methods:** From 54 TGF- $\beta$ -related genes, this research determined the genes showing the greatest relation to LIHC prognosis, and developed a risk score model with 8 TGF- $\beta$ -related genes. The model divided LIHC patients from different datasets and platforms into low- and high-risk groups. Multivariate Cox regression analysis confirmed that the model was an independent prognostic factor for LIHC. The differences in genetic mutation, immune cell infiltration, biological pathway, response to immunotherapy or chemotherapy, and tumor microenvironment in LIHC samples showing different risks were analyzed.

**Results:** Compared with low-risk group, in the training set and test set, high-risk group showed shorter survival, lower stromal score and higher M0 macrophages scores, regulatory T cells (Tregs), helper follicular T cells. Moreover, high-risk samples showed higher sensitivity to cisplatin, imatinib, sorafenib and salubrinal and pyrimethamine. High-risk group demonstrated a significantly higher Tumor Immune Dysfunction and Exclusion (TIDE) score, but would significantly benefit less from taking immunotherapy and was less likely to respond to immune checkpoint inhibitors.

**Conclusions:** In general, this work provided a risk scoring model based on 8 TGF- $\beta$  pathway-related genes, which might be a new potential tool for predicting LIHC.

**Keywords:** TGF- $\beta$  signaling pathway, Liver hepatocellular carcinoma, Tumor microenvironment, Prognosis, immunotherapy

## Background

In 2020, primary liver cancer was the third major cause resulting in cancer death worldwide, with morbidity and

mortality rates 2–3 times higher in men than in women in most regions. Liver hepatocellular carcinoma (LIHC) is the most common primary liver cancer [1]. Although several staging systems, such as the Barcelona Clinic Liver Cancer (BCLC) system, Cancer of the Liver Italian Program (CLIP), TNM, Okuda, Japanese Integrated Staging (JIS) Score, have been developed to treat LIHC, but they all have some limitations that cannot be neglected [2]. The Barcelona Clinic Liver Cancer (BCLC) system,

\*Correspondence: 3157882462@qq.com

<sup>2</sup> Department of Medical Oncology, Dongguan Institute of Clinical Cancer Research, 78 Wandao Road, Dongguan City 523000, Guangdong Province, China

Full list of author information is available at the end of the article



© The Author(s) 2022. **Open Access** This article is licensed under a Creative Commons Attribution 4.0 International License, which permits use, sharing, adaptation, distribution and reproduction in any medium or format, as long as you give appropriate credit to the original author(s) and the source, provide a link to the Creative Commons licence, and indicate if changes were made. The images or other third party material in this article are included in the article's Creative Commons licence, unless indicated otherwise in a credit line to the material. If material is not included in the article's Creative Commons licence and your intended use is not permitted by statutory regulation or exceeds the permitted use, you will need to obtain permission directly from the copyright holder. To view a copy of this licence, visit <http://creativecommons.org/licenses/by/4.0/>. The Creative Commons Public Domain Dedication waiver (<http://creativecommons.org/publicdomain/zero/1.0/>) applies to the data made available in this article, unless otherwise stated in a credit line to the data.

which was endorsed by European and American clinical practice guidelines, guides treatment choices and provides patients' survival information [3]. Reasonable method for the diagnosis and treatment of LIHC has been developed, according to the BCLC stage. Application of these methods to comprehensive projects in high-risk populations has shown a great effectiveness in preventing LIHC and reducing overall mortality [4]. Development of new therapies and their combinations for treating adjuvant and intermediate-stage disease, discovery of biomarkers for therapeutic purpose could help treat LIHC [5].

Transforming growth factor-beta (TGF- $\beta$ ) signaling is present in initial liver injury to inflammation and fibrosis, to cirrhosis and LIHC [6]. During the development of LIHC, TGF- $\beta$  has different effects on each stage of LIHC development. Early TGF- $\beta$  inhibits liver tumorigenesis through inducing cell arrest and apoptosis, but once cells get rid of its inhibition, TGF- $\beta$  develops the characteristics of migratory tumor initiation cells and promotes more advanced malignant progression via inducing cancer cell epithelial-mesenchymal transition (EMT), migration, invasion and final metastasis [7, 8]. Therefore, targeting TGF- $\beta$  pathway might treat LIHC and help understand the potential pathogenetic mechanisms, with a special focus on the crosstalk between other signaling pathways and TGF- $\beta$  [9]. Novel drugs that block TGF- $\beta$  pathway have entered clinical evaluation, among which the most advanced is LY2157299, which has been confirmed in phase I studies to have antitumor activity in patients suffering from advanced LIHC through mainly affecting cancer cell migration and invasion [10]. In view of the dual role of TGF- $\beta$ , there are still many factors hindering TGF- $\beta$  inhibitors development, particularly patient selection, timing of treatment and predictive biomarkers [11].

In this study, TGF- $\beta$  pathway-related genes from the Public Molecular Signature Database v7.4 (MSigDB) [12] were used to study the prognostic value of their expression profile in LIHC. Based on TGF- $\beta$  pathway-related genes, a risk score model was designed for exploring the differences between different risk groups among immune cell infiltration, genetic changes, tumor microenvironment, response to immunotherapy or chemotherapy, function. A risk score model based on TGF- $\beta$  pathway-related genes may be a promising tool for monitoring LIHC.

## Methods

### Acquisition of TGF- $\beta$ pathway-related genes

A gene set within TGF- $\beta$  pathway with suppressing, driving or mark function were obtained from MSigDB (v7.4).

After removing duplicates, a total of 54 TGF- $\beta$  pathway-related genes were retained for further analysis (Supplementary Table S1).

### Data acquisition of LIHC

LIHC data with clinical information, gene expression profiles and gene mutation data were acquired from three public databases, including The Cancer Genome Atlas database (TCGA, <https://portal.gdc.cancer.gov/>), Gene Expression Omnibus database (GEO, <https://www.ncbi.nlm.nih.gov/geo/>) and hepatocellular carcinoma database (HCCDB, <http://lifeome.net/database/hccdb/home.html>). TCGA-LIHC dataset including RNA sequencing (RNA-seq) data, gene mutation data, and clinical information was downloaded from TCGA database [13]. GSE10143 [14], GSE14520 [15] and GSE76427 [16] datasets containing gene expression profiles (microarray data) and clinical information were acquired from GEO database. ICGC-LIRI-JP dataset (named as ICGC (International Cancer Genome Consortium) in the following) containing RNA-seq data and clinical information was downloaded from HCCDB.

### Data preprocessing of LIHC

For LIHC samples in these datasets, samples without survival time, survival status or follow-up data were excluded. For RNA-seq data in TCGA-LIHC and ICGC datasets, Ensembl ID was converted to gene symbol. Averaged expression value was selected for one gene with multiple gene symbols. For gene expression profiles in GSE datasets, gene probes were converted to gene symbol. Probes targeting multiple genes were excluded. Averaged expression was used when multiple probes corresponding to one gene. Finally, after data preprocessing, 365 samples (130 censored and 235 uncensored, with the longest follow-up time of 10.0 years (only numbers were shown in the following)) from TCGA-LIHC dataset remained. 80 (32, 48, 15.6), 221 (85, 136, 5.5), and 115 (23, 92, 6.5) samples from GSE10143, GSE14520 and GSE76427 datasets remained, respectively. 203 samples (35, 138, 5.9) from ICGC dataset (Supplementary Table S2) remained. TCGA-LIHC dataset was set as a training dataset, and the other four datasets were independent dataset.

### Development of a prognostic gene signature

Firstly, univariate Cox regression analysis was conducted to determine prognosis-associated TGF- $\beta$  pathway-related genes in TCGA-LIHC dataset. Least absolute shrinkage and selection operator (LASSO) Cox regression analysis in glmnet (v4.1) package [17] was performed to shrink the number of prognostic genes and construct an optimal prognostic model. LASSO allows

a shrinkage estimation and construction of a simplified model with penalty function. The coefficients of prognostic genes were compressed by increasing lambda values. The optimal lambda value was confirmed by 95% confidence interval (CI) and examined by 10-fold cross-validation. Eight prognostic genes were identified with the optimal lambda value. Then the prognostic model was developed according to the expression of each gene and gene coefficients obtained from LASSO Cox regression. The risk model was defined as: risk score =  $\sum$  (coefficient  $i$  \* expression  $i$ ), where  $i$  indicated each gene.

Next, risk score for each sample was calculated, and samples were stratified into low- and high-risk groups according to the optimal cut-off value determined by `surv_cutpoint` function in `survminer` (v0.4.9) R package (<https://cran.r-project.org/web/packages/survminer/index.html>). Independent cut-off value of each dataset was calculated using the same algorithm. Kaplan-Meier survival analysis was conducted for measuring overall survival (OS) between high- and low-risk groups (log-rank test was performed). The effectiveness of the model was evaluated by receiver operating characteristic (ROC) analysis in `timeROC` (v0.4) R package [18]. Area under ROC curve (AUC) was calculated for assessing the performance of the prognostic model in each dataset.

#### Gene set enrichment analysis (GSEA)

GSEA software (v4.2.0) developed by UC San Diego and Broad Institute (<https://www.gsea-msigdb.org/gsea/index.jsp>) was applied to further analyze enriched biological pathways of the two risk groups in TCGA-LIHC dataset [19]. A gene set of KEGG pathways “c2.cp.kegg.v7.4.symbols.gmt” was downloaded from MSigDB (<https://www.gsea-msigdb.org/gsea/msigdb/index.jsp>, v7.4) [12]. DESeq2 (v1.34) was employed to normalize RNA-seq data and produce a GSEA compatible “normalized counts” table in the gene cluster text (GCT) format [20]. Then normalized expression data grouped by risk groups was used as an input for conducting GSEA. Significantly enriched pathways with  $P < 0.05$  were considered as significant.

#### Gene mutation analysis for two risk groups

Gene mutation data in TCGA-LIHC dataset included tumor mutation burden (TMB), number of mutated genes, and single nucleotide variations (SNVs), which was already processed using `mutect2` (v4.1.0.0) tool in The Genome Analysis Toolkit (GATK, <https://gatk.broadinstitute.org/hc/en-us/articles/360037593851-Mutect2>) by TCGA research group [21]. Student  $t$  test was applied for comparing TMB and number of mutated genes between high- and low-risk groups.  $P < 0.05$  was considered as significant. *Chi-square* test

was conducted for screening significantly mutated genes in the two risk groups ( $P < 0.05$ ). The top 10 mutated genes were visualized by waterfall plot.

#### Estimation of tumor microenvironment and immune cells

RNA-seq data of TCGA-LIHC were uploaded into Cell type Identification By Estimating Relative Subsets Of RNA Transcripts (CIBERSORT, <https://cibersort.stanford.edu/>) tool to evaluate the infiltration of 22 immune cells in the tumor microenvironment, including naïve and memory B cells, seven T cell types, plasma cells, myeloid subsets, and natural killer (NK) cells [22]. The scores of these immune cells between the two risk groups were compared by Wilcoxon test. In addition, Estimation of STromal and Immune cells in MAlignant Tumours using Expression data (ESTIMATE, v1.0.13) package was introduced to calculate ESTIMATE score, stromal score, and immune score, through indicating the fraction of immune and stromal cells in tumor samples using gene expression signatures [23].

#### Prediction of immune/chemotherapy response

Based on modeling tumor immune evasion mechanism, the response to immunotherapy could be predicted by Tumor Immune Dysfunction and Exclusion (TIDE) tool [23]. To initially evaluate the response of two risk groups in the TCGA-LIHC dataset to immunotherapy, the TIDE algorithm was used. To further measure the response of each risk group to immunotherapy, we used subclass mapping (SubMap) analysis for comparing anti-programmed cell death ligand 1 (PD-L1) therapy response of the IMvigor210 dataset with that of TCGA-LIHC [24]. Furthermore, the half maximal inhibitory concentration (IC50) value of five chemotherapy or targeted drugs (imatinib, sorafenib, cisplatin, salubrinal and pyrimethamine) [25] for each sample in TCGA-LIHC dataset was evaluated by `pRRophetic` package [26].

#### Statistical analysis

R software (v4.1) was employed for all statistical analysis. Survival R package (<https://mran.microsoft.com/web/packages/survival/index.html>) was utilized to perform Kaplan-Meier survival analysis, univariate and multivariate Cox regression analysis (log-rank test was conducted). The association of seven metagenes with the risk score was assessed by Pearson correlation analysis [27]. Differences between the two risk groups were analyzed by Wilcoxon test or student  $t$  test (indicated in the

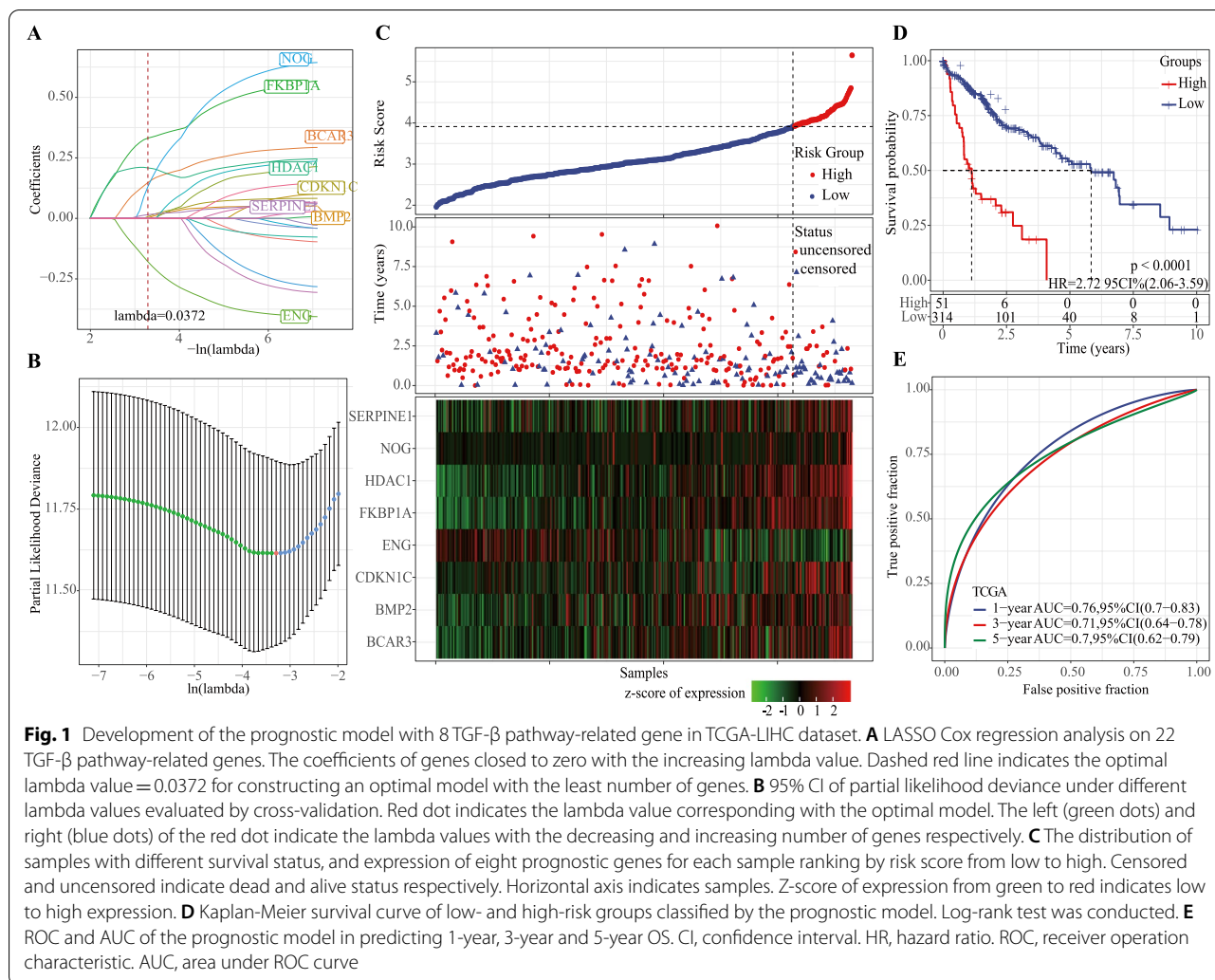


figure legends). If not specified,  $P < 0.05$  was considered as significant.

## Results

### Development of the prognostic model

The univariate Cox regression analysis of 54 TGF-β pathway-related gene was carried out with TCGA-LIHC dataset as training set to identify the prognostic TGF-β pathway-related genes in LIHC. The results showed that the expression levels of 22 TGF-β pathway-related genes were significantly correlated with the OS of LIHC. Then LASSO Cox regression analysis was performed to screen the most stable prognostic genes from the 22 TGF-β pathway-related genes. Partial likelihood deviance was the minimum when 8 variables were included in the model (Fig. 1A, B). Finally, TGF-β pathway risk score formula was constructed, according to 8 TGF-β pathway-related genes as risk score =  $0.073 \times CDKN1C + 0.18 \times HDAC1 + 0.035 \times SER-$

$PINE1 + 0.068 \times BMP2 - 0.372 \times ENG + 0.392 \times FKBP1A + 0.481 \times NOG + 0.279 \times BCAR3$ . This formula was introduced to calculate the risk score of TCGA-LIHC samples and effectively distinguished the survival status of patients with different risks (Fig. 1C). 51 samples and 314 samples were classified into high- and low-risk groups, respectively, based on the optimal cut-off value (Supplementary Table S3). High-risk scored patients showed a significantly more unfavorable prognosis than patients with low-risk scores (Fig. 1D). For TCGA-LIHC dataset, AUC of risk score for predicting 1-year, 3-year, and 5-year OS was 0.76, 0.71, and 0.70, respectively (Fig. 1E).

### Validation of the prognostic model in the GEO and ICGC datasets

To analyze the robustness of the model established based on TCGA-LIHC dataset, the risk scores of the samples were calculated by the same risk score

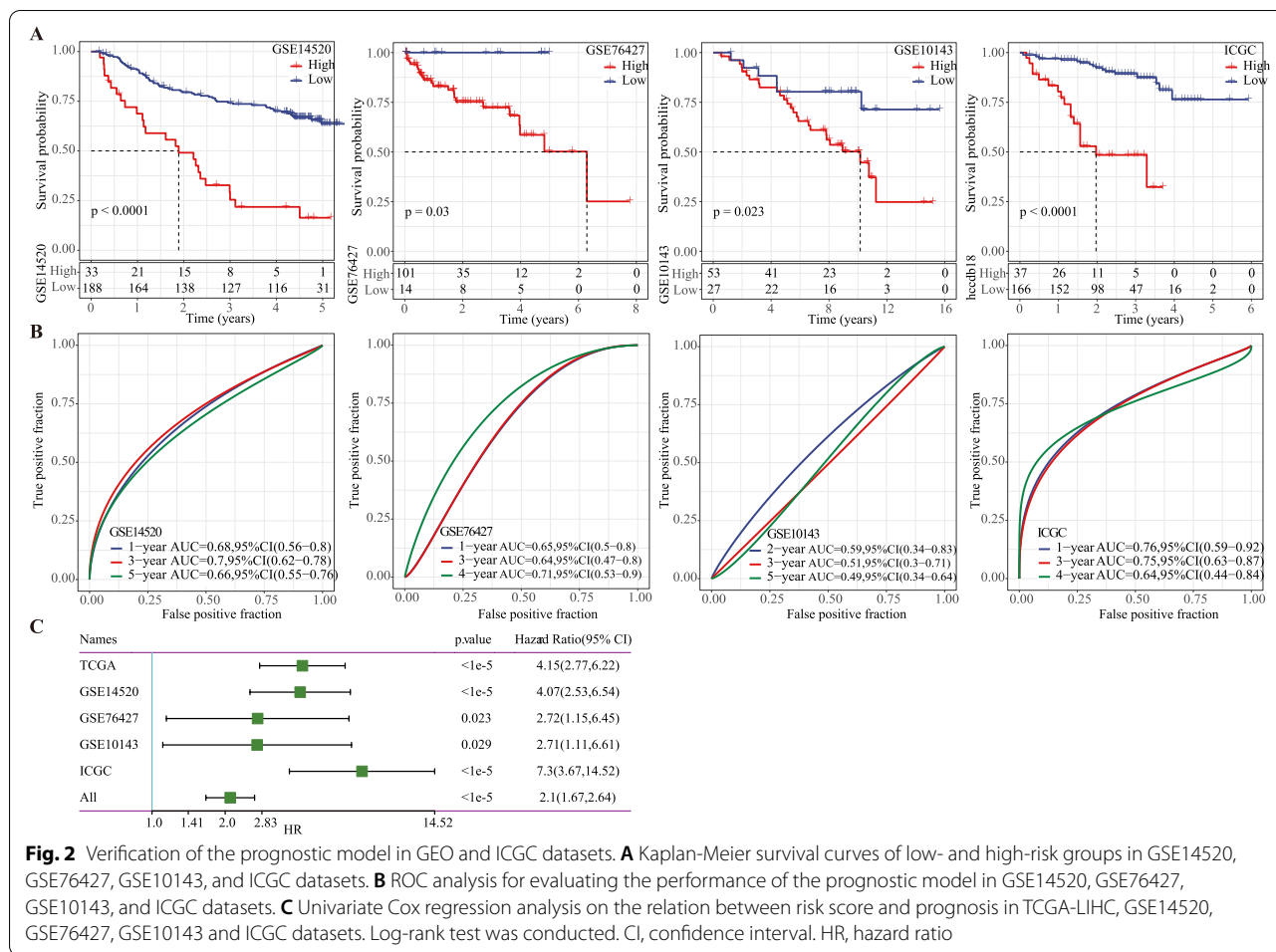


**Fig. 2** Verification of the prognostic model in GEO and ICGC datasets. **A** Kaplan-Meier survival curves of low- and high-risk groups in GSE14520, GSE76427, GSE10143, and ICGC datasets. **B** ROC analysis for evaluating the performance of the prognostic model in GSE14520, GSE76427, GSE10143, and ICGC datasets. **C** Univariate Cox regression analysis on the relation between risk score and prognosis in TCGA-LIHC, GSE14520, GSE76427, GSE10143 and ICGC datasets. Log-rank test was conducted. CI, confidence interval. HR, hazard ratio

formula. GSE14520, GSE76427, GSE10143 and ICGC were the external validation datasets. According to optimum cut-off values, LIHC samples in each dataset were grouped into two risk groups (Supplementary Table S3). Samples classified as high-risk were more likely to be in a death status, as demonstrated by the survival analysis of the samples in each dataset (Fig. 2A). The ROC curve showed that the prognostic model had a 3-year AUC values of 0.7 in GSE14520, 0.64 in GSE76427, 0.51 in GSE10143 and 0.75 in ICGC (Fig. 2B). Correlation of the OS of LIHC with the risk score of each dataset was also assessed by univariate Cox regression, and the risk score was

found to be closely linked with OS in all the five datasets (Fig. 2C).

### Genetic variation and functional enrichment analysis of the prognostic risk model

Between the high- and low-risk groups, statistical analysis of TMB and nucleotide variation was not significantly different in TMB or nucleotide variation (Fig. 3A, B). In these two risk groups, single nucleotide variations in genes with the top 10 mutation frequencies were exhibited in Fig. 3C. The highest mutation frequency was present in TP53, the mutation rate of which was much higher than CSMD1 showing the second highest

(See figure on next page.)

**Fig. 3** Gene mutation features and gene set enrichment analysis in TCGA-LIHC datasets. **A-B** Comparison of TMB (A) and number of mutated genes (B) between low- and high-risk groups. Student *t* test was conducted. **C** The waterfall diagram visualizing the top 10 mutated genes in the two risk groups ( $P < 0.05$ ). *Chi*-square test was performed. **D** Enriched four KEGG pathways in low-risk group assessed by gene set enrichment analysis. TMB, tumor mutation burden. ES, enrichment score. NES, normalized enrichment score. FDR, false discovery rate. ns, no significance



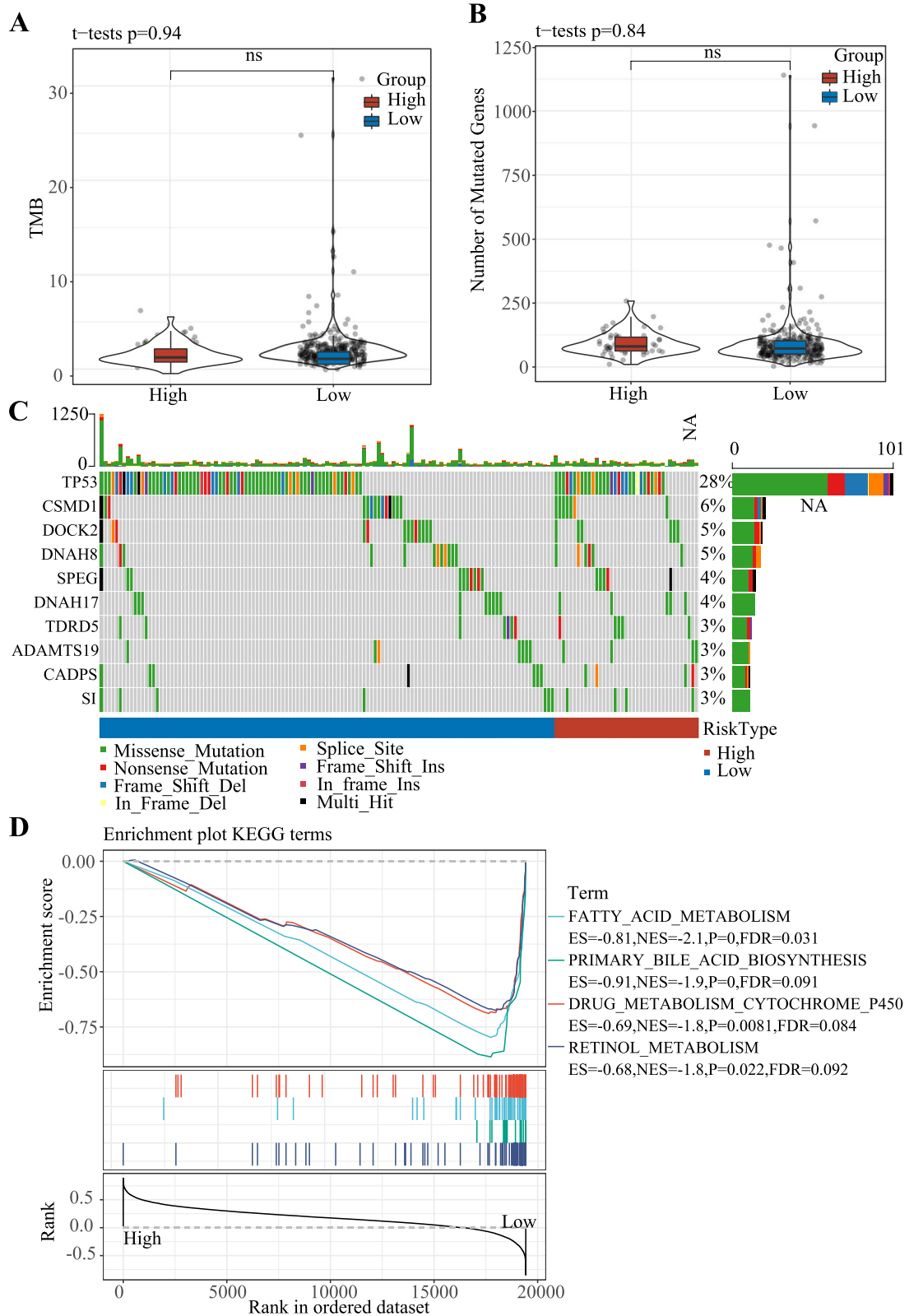


**Fig. 3** (See legend on previous page.)

mutation frequency. GSEA on the two risk groups in TCGA-LIHC dataset revealed that metabolism-related pathways, including primary bile acid biosynthesis, fatty acid metabolism, retinol metabolism, and drug metabolism cytochrome P450, were significantly enriched in low-risk group, suggesting that the risk model can predict patient survival by reflecting LIHC metabolism (Fig. 3D).

#### Correlation between risk score and clinical features

In different subgroups, risk scores stratified by M stage, gender, age, N stage, American Joint Committee on Cancer (AJCC) stage, grade, T stage were compared. High-risk scored patients were more likely to be those with a more advanced T stage ( $P=1.1e-05$ ), and a high histological grade ( $P=6e-07$ ) and AJCC stage ( $P=9.3e-06$ ) in comparison with those showing low-risk scores (Fig. 4A). In addition, samples could be significantly stratified into the two risk groups of different clinical features, including gender (male and female), T stage (T1–2 and T3–4), age (age > 60 and age ≤ 60), AJCC stage (stage I–II and stage III–IV), and M stage (M0 stage), N stage (N0 stage) and grade (G1–G2 and G3–G4) (Fig. 4B). The LIHC samples showing a high-risk had generally significantly worse OS than low-risk patients, indicating that the risk model had strong predictive ability (Fig. 4B). Risk score, AJCC stage, T stage were noticeably associated with LIHC prognosis, as shown by univariate Cox regression analysis (Fig. 5A). After controlling confounding factors, multivariate Cox regression study demonstrated that the risk model was the only independent prognostic factor for LIHC (Fig. 5B).

#### Tumor microenvironment and immune cells in each risk group

To better understand the immune microenvironment traits associated with the risk model developed based on 8 TGF- $\beta$  pathway-related genes, the ESTIMATE, stromal and immune scores of each risk group were calculated by ESTIMATE. Stromal score was significantly lower in the high-risk group than low-risk group, while ESTIMATE score and immune score of the two risk groups showed no significant difference, suggesting that the high-risk group had a relatively low stromal component (Fig. 6A–C). Moreover, the difference analysis on the composition of 22 immune cells in the tumor microenvironment between the two risk groups demonstrated a significant difference in 9 immune cells (Fig. 6D, E). High-risk group showed a higher infiltration of helper follicular T cells, M0 macrophages, and regulatory T cells (Tregs), while resting memory CD4 T cells, monocytes, resting mast cells, M1 macrophages were more significantly enriched in low-risk group (Fig. 6E). Because of the linkage effect between cancer immunity and inflammation, 7

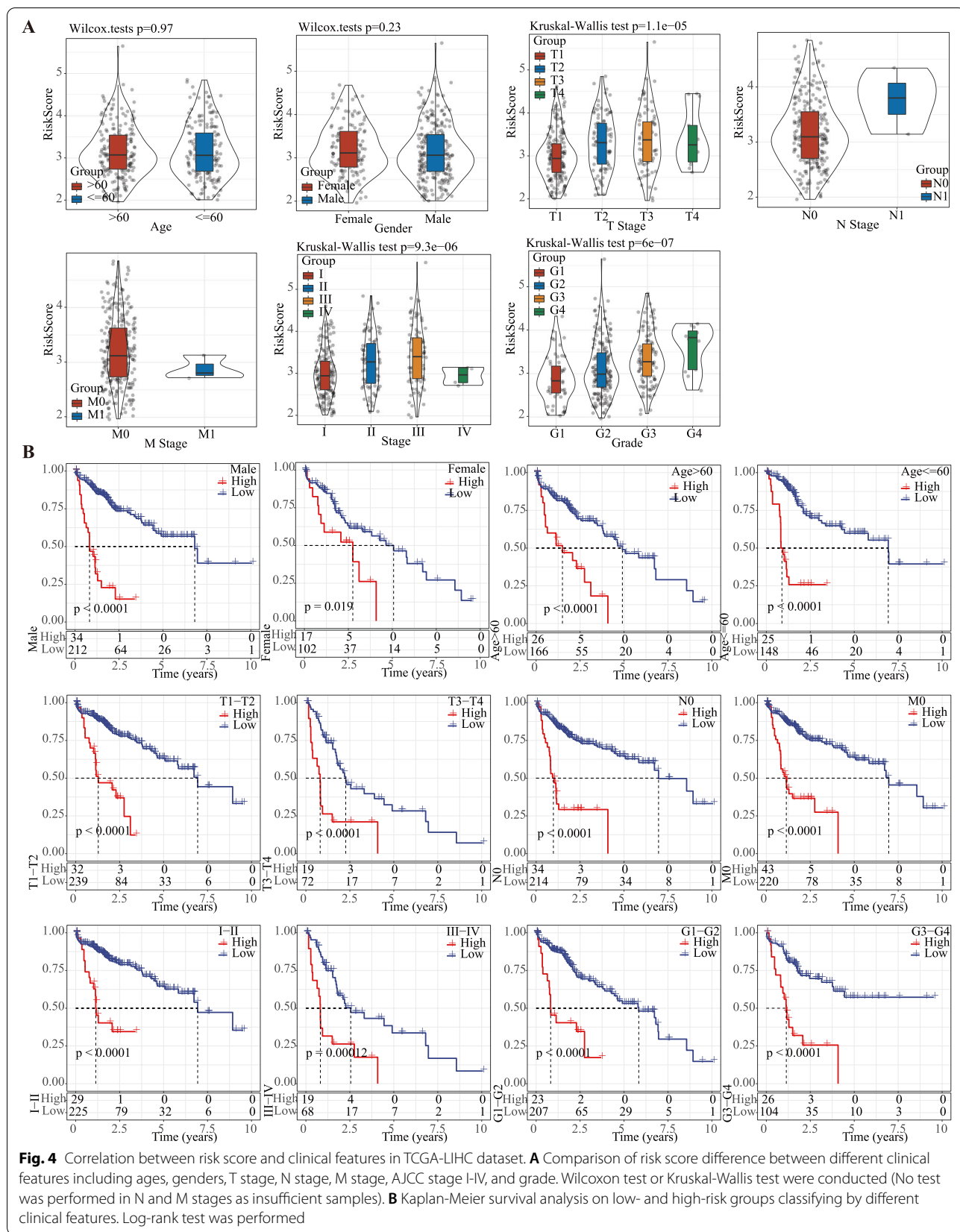
metagenes (including 105 genes related to inflammation and immune functions) was selected to calculate enrichment score by single sample gene set enrichment analysis (ssGSEA) in gene set variation analysis (GSVA) package. Risk score was negatively correlated with interferon and MHC- I ( $R=-0.2$  and  $-0.14$ , respectively) but positively correlated with IgG ( $R=0.25$ ), as shown by correlation analysis (Fig. 6F). Although the correlations were not strong, a significant difference of ssGSEA score was shown on IgG, interferon, and MHC-I between the two risk groups in a boxplot ( $P<0.05$ , Fig. 6G).

#### Risk model based on 8 TGF- $\beta$ pathway -related genes could predict the clinical response of immunotherapy/ chemotherapy

Between the two risk groups, the difference in the score of infiltrating immune cell populations in tumor microenvironment indicated that the response of each risk group to immunotherapy required further exploration. The TIDE algorithm was utilized to analyze the response rate of immunotherapy of the two groups (Fig. 7A). Low-risk patients had significantly higher remission after taking immunotherapy than the high-risk. Moreover, TIDE score of low-risk patients was greatly lower (Fig. 7B). From the Submap analysis, it could be found that the low-risk group was more likely to respond to anti-PD-L1 treatment (Fig. 7C). The cisplatin, imatinib, sorafenib, salubrinal and pyrimethamine treatment-related IC50 in TCGA-LIHC samples was estimated to evaluate the sensitivity of the two risk groups to these drugs, and we found that high-risk LIHC samples were more sensitive to the above five drugs (Fig. 7D–H).

#### Discussion

It is widely acknowledged that LIHC treatment is challenging for its high possibility of drug resistance. The development of clinically validated agents against LIHC has been significantly influenced by the complex interactions of liver tumors with their immune microenvironment and a lack of understanding of the heterogeneous mechanisms of LIHC tumorigenesis and progression [28]. Several studies have shown that dysregulated signals in the TGF- $\beta$  pathway have important function in immune regulation in the LIHC microenvironment [8, 11]. Therefore, TGF- $\beta$  pathway-targeted drugs, including drugs targeting TGF- $\beta$  ligands, TGF- $\beta$  receptors, and downstream mediators of TGF- $\beta$ , have been explored and clinically tested. And all of those drugs can lead to a variety of synergistic downstream effects and may improve the clinical outcome of LIHC [29, 30]. At present, effective biomarkers should be discovered to help determine the response of tumor cells for LIHC patients [31].





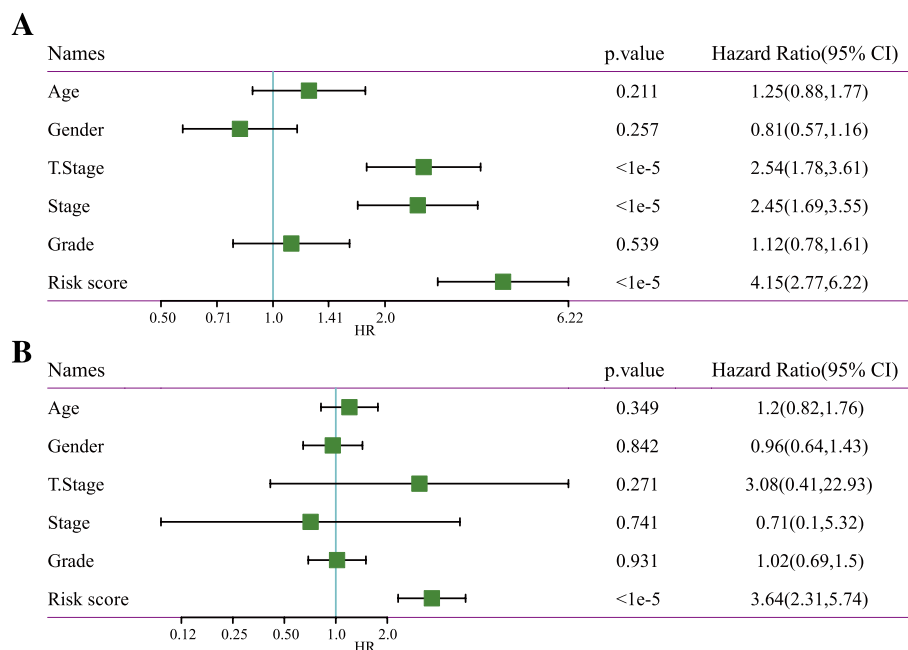


**Fig. 5** Univariate (A) and multivariate (B) Cox regression analysis for risk score and clinical features including age, gender, T stage, stage, and grade in TCGA-LIHC dataset. Log-rank test was performed. CI, confidence interval. HR, hazard ratio

This work developed a risk score model based on 8 TGF- $\beta$  pathway-related genes through progressively screening 54 TGF- $\beta$  pathway-related genes, which can score and group LIHC samples in independent datasets. Chen et al. found that about 40% of all LIHC samples showed at least one gene mutation in the TGF- $\beta$  pathway [32]. In the high- and low-risk groups, TP53 was both identified to have the highest mutation frequency, which has been identified as a common molecular event in human liver cancer [33]. Previous studies have suggested that with the continuous acquisition of genomic mutations, tumor cells show a series of mutations in different signal pathways, resulting in changes in TGF- $\beta$  response [34]. This also explained the function of TGF- $\beta$  in the late stage of tumor was quite different from that in the early stage. In addition, GSEA showed that two risk groups had differential enriched pathways such as metabolism-related pathways like fatty acid metabolism, and drug metabolism were more enriched in low-risk group, which may be resulted from their differential mutation patterns in TP53 and metabolism-related genes.

A number of evidences show that TGF- $\beta$  can modulate cellular responses that regulate the tumor microenvironment, which may also contribute to LIHC progression and drive immune escape of cancer cells [31]. On the comparison of tumor microenvironment and immune infiltration between two risk groups, we found that high-risk group had relatively higher enrichment of helper

follicular T cells, Tregs and M0 macrophages. The previous study speculated that increased number of these immunosuppressive cells endowed high-risk group a strong immunosuppressive environment, leading to an unfavorable prognosis [34]. Importantly, two risk groups showed significantly different response to immunotherapy, where TIDE score of low-risk group was noticeably lower and responsive proportion was significantly higher, suggesting that low-risk group may be more responsive to anti-PD-L1 treatment. However, high-risk group was more sensitive to chemotherapeutic drugs or targeted drugs including cisplatin, imatinib, sorafenib and salubrinal and pyrimethamine. These observations suggested that the prognostic model had a potential in guiding immunotherapy or targeted therapy for LIHC patients.

Eight prognostic genes (CDKN1C, HDAC1, SERPINE1, BMP2, ENG, FKBP1A, NOG, and BCAR3) involved in TGF- $\beta$  pathway were included in our prognostic model. We found that some of them were also identified as prognostic biomarkers for cancers by the previous studies. Cyclin-dependent kinase inhibitor 1C (CDKN1C, also known as p57(KIP2)), a tumor suppressor, could regulate tumor cell differentiation, invasion, and angiogenesis, which is also validated as a prognostic biomarker in various cancer types, including in LIHC [35, 36]. In a 7-gene hypoxia signature developed by Bai et al., CDKN1C has also been identified as a prognostic gene for predicting LIHC prognosis [37]. Histone deacetylase 1 (HDAC1)

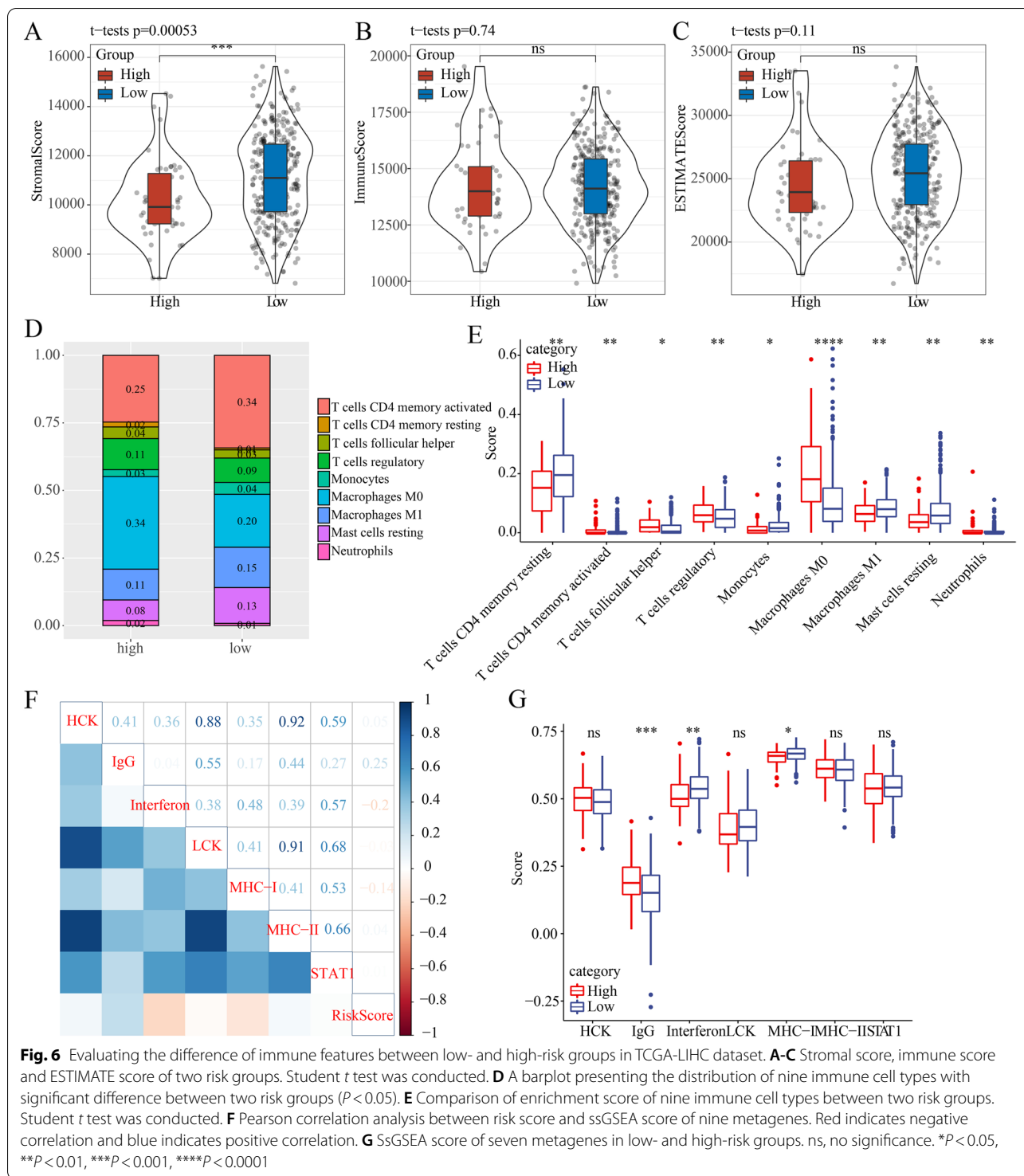
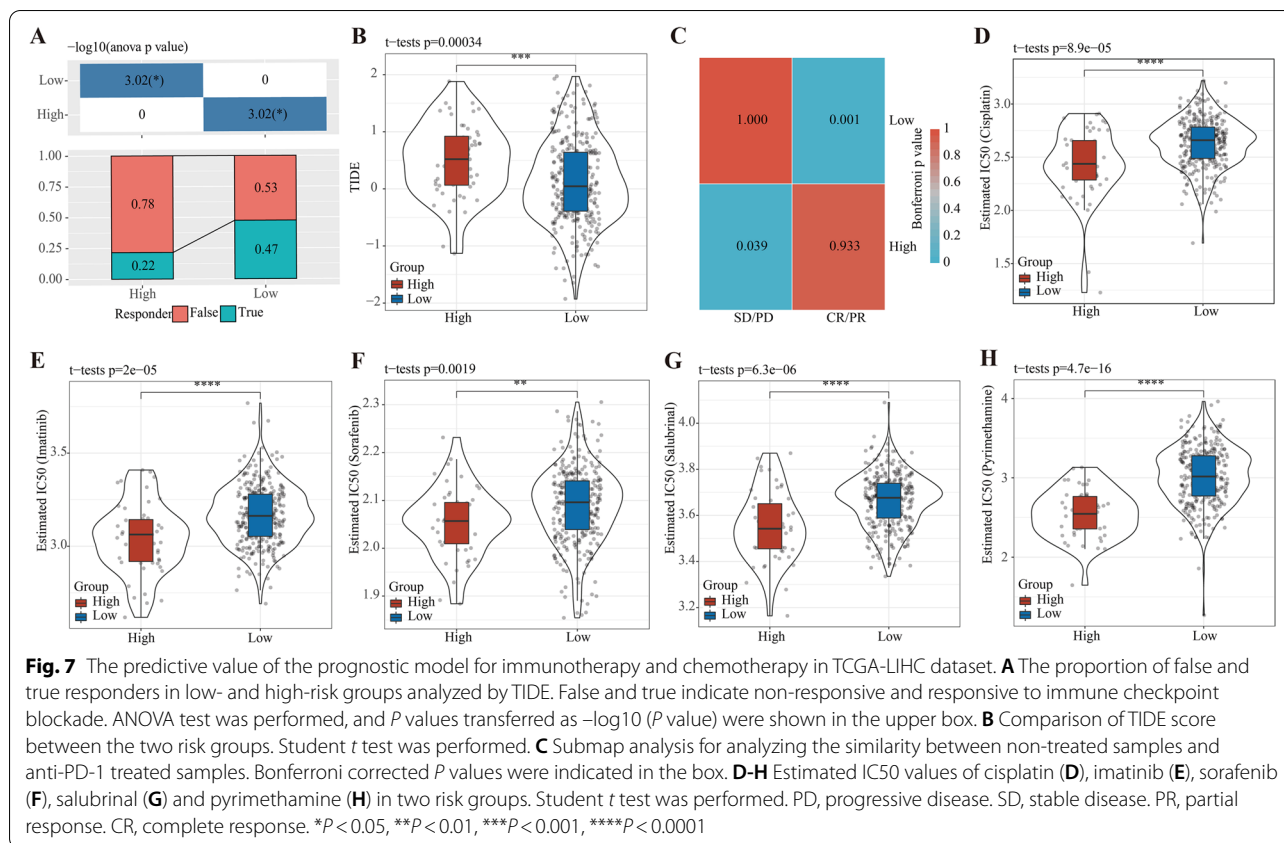


**Fig. 6** Evaluating the difference of immune features between low- and high-risk groups in TCGA-LIHC dataset. **A-C** Stromal score, immune score and ESTIMATE score of two risk groups. Student *t* test was conducted. **D** A barplot presenting the distribution of nine immune cell types with significant difference between two risk groups ( $P < 0.05$ ). **E** Comparison of enrichment score of nine immune cell types between two risk groups. Student *t* test was conducted. **F** Pearson correlation analysis between risk score and ssGSEA score of nine metagenes. Red indicates negative correlation and blue indicates positive correlation. **G** SsGSEA score of seven metagenes in low- and high-risk groups. ns, no significance. \* $P < 0.05$ , \*\* $P < 0.01$ , \*\*\* $P < 0.001$ , \*\*\*\* $P < 0.0001$

is a critical enzyme for epigenetic modification, whose overexpression is strongly correlated with tumor cell proliferation and growth in many cancers [38]. High expression of HDAC1 is significantly associated with elevated cancer-specific mortality in LIHC [39]. Plasminogen

activator inhibitor 1 (SERPINE1, also known as PAI-1), is considered as a prognostic biomarker for gastric cancer, gliomas, and colorectal cancer [40–42], hepatocellular carcinoma [43]. SERPINE1 was also in an 8-gene prognostic by Lin et al [44] High expression of bone



morphogenetic protein 2 (BMP2) could promote liver cancer cell growth through activating myeloid-derived suppressor cells [45]. Other four prognostic genes were less reported in LIHC research.

The 8-gene prognostic model manifested favorable performance in different datasets, except in GSE10143 dataset with an unsatisfied AUC. Nevertheless, our model still outperformed other present prognostic models for LIHC in the same datasets (TCGA-LIHC and ICGC). 1-year, 3-year and 5-year AUC were 0.76, 0.71 and 0.70 in TCGA-LIHC dataset, respectively. 1-year, 3-year and 4-year AUC were 0.76, 0.75 and 0.64 in ICGC dataset, respectively. We included some studies containing at least one prognostic gene as our model. Sun et al. established a 2-gene prognostic model (CANX and HDAC1) for LIHC based on immune-related and autophagy-related genes using TCGA-LIHC and ICGC datasets [46]. The AUC of the 2-gene prognostic model for 1-year, 3-year and 5-year were 0.696, 0.639 and 0.642 in TCGA training dataset, 0.728, 0.685 and 0.612 in TCGA test dataset, 0.757, 0.669 and 0.644 in ICGC dataset, respectively. Lin et al. constructed an 8-gene prognostic model (SLC7A1, RIPK2, NOD2, ADORA2B, MEP1A, ITGA5, P2RX4, and SERPINE1) based on inflammatory response-related genes for LIHC also

utilizing TCGA-LIHC and ICGC datasets [44]. The AUC of Lin et al's model for predicting 3-year OS was 0.614 and 0.710 in TCGA-LIHC and ICGC datasets, respectively [44]. Compared with other prognostic models, our model was validated in more datasets, while they only validated their models in ICGC dataset.

This study had some limitations. Firstly, all the data were retrospective data, and experiments were not designed to verify them from other aspects. Secondly, our analysis was only based on TGF- $\beta$  pathway-related genes, and the results did not represent all LIHC-related gene profiles. Thirdly, algorithms for characterizing tumor microenvironment, such as ESTIMATE and CIBERSORT, are not always accurate due to the atypical or unclear tumor microenvironment varying by tumor types. There was a possibility that an overlap of some gene signatures may exist between stromal cells and tumor cells because of the influence of epithelial-to-mesenchymal transition (EMT). In the future, the scope of research should be further expanded and experimental studies should be carried out to analyze the risk model based on TGF- $\beta$  pathway-related genes on LIHC pathological behavior.

## Conclusions

In conclusion, a risk score model with stepwise analysis of 54 TGF- $\beta$  pathway-related genes in TCGA-LIHC was developed, which can independently predict the LIHC prognosis and was related to the response to immunotherapy or chemotherapy, immune cell infiltration, tumor microenvironment. This study provided a perspective to elucidate LIHC clinical outcomes from the perspective of TGF- $\beta$  pathway-related genes, offering novel possibility for improving LIHC management.

## Supplementary Information

The online version contains supplementary material available at <https://doi.org/10.1186/s12953-022-00192-4>.

**Additional file 1: Supplementary Table S1.** A list of 54 TGF- $\beta$  pathway-related genes.

**Additional file 2: Supplementary Table S2.** Clinical features of the LIHC samples in different datasets.

**Additional file 3: Supplementary Table S3.** Classification of low- and high-risk groups in five datasets.

## Acknowledgements

Not applicable

## Authors' contributions

All authors contributed to the study conception and design. Material preparation, data collection and analysis were performed by QL, JTC, ZBL, and HTM. The first draft of the manuscript was written by JSL and JJ commented on previous versions of the manuscript. All authors read and approved the final manuscript.

## Funding

Not applicable.

## Availability of data and materials

The datasets generated during and/or analysed during the current study are available in the [GSE14520] repository, [<https://www.ncbi.nlm.nih.gov/geo/query/acc.cgi?acc=GSE14520>]; in [GSE76427] repository, [<https://www.ncbi.nlm.nih.gov/geo/query/acc.cgi?acc=GSE76427>]; in [GSE10143] repository, [<https://www.ncbi.nlm.nih.gov/geo/query/acc.cgi?acc=GSE10143>].

## Declarations

### Ethics approval and consent to participate

Not applicable.

### Consent for publication

Not applicable.

### Competing interests

The authors declare that they have no competing interests.

### Author details

<sup>1</sup>Department of Medical Oncology, Affiliated Dongguan Hospital, Southern Medical University, 78 Wandao Road, Dongguan City 523000, Guangdong Province, China. <sup>2</sup>Department of Medical Oncology, Dongguan Institute of Clinical Cancer Research, 78 Wandao Road, Dongguan City 523000, Guangdong Province, China.

Received: 21 October 2021 Accepted: 6 May 2022

Published online: 22 June 2022

## References

- Sung H, et al. Global Cancer statistics 2020: GLOBOCAN estimates of incidence and mortality worldwide for 36 cancers in 185 countries. *CA Cancer J Clin*. 2021;71:209–49. <https://doi.org/10.3322/caac.21660>.
- Vogel A, et al. Hepatocellular carcinoma: ESMO clinical practice guidelines for diagnosis, treatment and follow-up. *Ann Oncol*. 2019;30:871–3. <https://doi.org/10.1093/annonc/mdy510>.
- Su TH, Hsu SJ, Kao JH. Paradigm shift in the treatment options of hepatocellular carcinoma. *Liver Int*. 2021. <https://doi.org/10.1111/liv.15052>. Epub ahead of print.
- Yang JD, et al. A global view of hepatocellular carcinoma: trends, risk, prevention and management. *Nat Rev Gastroenterol Hepatol*. 2019;16:589–604. <https://doi.org/10.1038/s41575-019-0186-y>.
- Fornier A, Reig M, Bruix J. Hepatocellular carcinoma. *Lancet*. 2018;391:1301–14. [https://doi.org/10.1016/S0140-6736\(18\)30010-2](https://doi.org/10.1016/S0140-6736(18)30010-2).
- Fabregat I, et al. TGF-beta signalling and liver disease. *FEBS J*. 2016;283:2219–32. <https://doi.org/10.1111/febs.13665>.
- Tu S, Huang W, Huang C, Luo Z, Yan X. Contextual regulation of TGF-beta signaling in liver Cancer. *Cells*. 2019;8:1235. <https://doi.org/10.3390/cells8101235>.
- Fabregat I, Caballero-Diaz D. Transforming growth factor-beta-induced cell plasticity in liver fibrosis and Hepatocarcinogenesis. *Front Oncol*. 2018;8:357. <https://doi.org/10.3389/fonc.2018.00357>.
- Arrese M, et al. TGF-beta and Hepatocellular carcinoma: when a friend becomes an enemy. *Curr Protein Pept Sci*. 2018;19:1172–9. <https://doi.org/10.2174/1389203718666171117112619>.
- Neuzillet C, et al. Perspectives of TGF-beta inhibition in pancreatic and hepatocellular carcinomas. *Oncotarget*. 2014;5:78–94. <https://doi.org/10.18632/oncotarget.1569>.
- Katz LH, et al. TGF-beta signaling in liver and gastrointestinal cancers. *Cancer Lett*. 2016;379:166–72. <https://doi.org/10.1016/j.canlet.2016.03.033>.
- Liberzon A, et al. The molecular signatures database (MSigDB) hallmark gene set collection. *Cell systems*. 2015;1:417–25. <https://doi.org/10.1016/j.cels.2015.12.004>.
- Cancer Genome Atlas Research Network. Comprehensive and Integrative Genomic Characterization of Hepatocellular Carcinoma. *Cell*. 2017;169:1327–1341.e1323. <https://doi.org/10.1016/j.cell.2017.05.046>.
- Hoshida Y, et al. Gene expression in fixed tissues and outcome in hepatocellular carcinoma. *N Engl J Med*. 2008;359:1995–2004. <https://doi.org/10.1056/NEJMoa0804525>.
- Roessler S, et al. A unique metastasis gene signature enables prediction of tumor relapse in early-stage hepatocellular carcinoma patients. *Cancer Res*. 2010;70:10202–12. <https://doi.org/10.1158/0008-5472.Ccr-10-2607>.
- Grinchuk OV, et al. Tumor-adjacent tissue co-expression profile analysis reveals pro-oncogenic ribosomal gene signature for prognosis of resectable hepatocellular carcinoma. *Mol Oncol*. 2018;12:89–113. <https://doi.org/10.1002/1878-0261.12153>.
- Simon N, Friedman J, Hastie T, Tibshirani R. Regularization paths for Cox's proportional hazards model via coordinate descent. *J Stat Softw*. 2011;39:1–13. <https://doi.org/10.18637/jss.v039.i05>.
- Blanche P, Dartigues JF, Jacqmin-Gadda H. Estimating and comparing time-dependent areas under receiver operating characteristic curves for censored event times with competing risks. *Stat Med*. 2013;32:5381–97. <https://doi.org/10.1002/sim.5958>.
- Subramanian A, et al. Gene set enrichment analysis: a knowledge-based approach for interpreting genome-wide expression profiles. *Proc Natl Acad Sci U S A*. 2005;102:15545–50. <https://doi.org/10.1073/pnas.0506580102>.
- Love MI, Huber W, Anders S. Moderated estimation of fold change and dispersion for RNA-seq data with DESeq2. *Genome Biol*. 2014;15:550. <https://doi.org/10.1186/s13059-014-0550-8>.
- Cibulskis K, et al. Sensitive detection of somatic point mutations in impure and heterogeneous cancer samples. *Nat Biotechnol*. 2013;31:213–9. <https://doi.org/10.1038/nbt.2514>.
- Chen B, Khodadoust MS, Liu CL, Newman AM, Alizadeh AA. Profiling Tumor Infiltrating Immune Cells with CIBERSORT. *Methods Mol Biol (Clifton, N.J.)*. 2018;1711:243–59. [https://doi.org/10.1007/978-1-4939-7493-1\\_12](https://doi.org/10.1007/978-1-4939-7493-1_12).

23. Yoshihara K, et al. Inferring tumour purity and stromal and immune cell admixture from expression data. *Nat Commun.* 2013;4:2612. <https://doi.org/10.1038/ncomms3612>.
24. Roh W, et al. Integrated molecular analysis of tumor biopsies on sequential CTLA-4 and PD-1 blockade reveals markers of response and resistance. *Sci Transl Med.* 2017;9:eaah3560. <https://doi.org/10.1126/scitranslmed.aah3560>.
25. Yang W, et al. Genomics of drug sensitivity in Cancer (GDSC): a resource for therapeutic biomarker discovery in cancer cells. *Nucleic Acids Res.* 2013;41:D955–61. <https://doi.org/10.1093/nar/gks1111>.
26. Geeleher P, Cox N, Huang RS. pRRophetic: an R package for prediction of clinical chemotherapeutic response from tumor gene expression levels. *PLoS One.* 2014;9:e107468. <https://doi.org/10.1371/journal.pone.0107468>.
27. Rody A, et al. T-cell metagene predicts a favorable prognosis in estrogen receptor-negative and HER2-positive breast cancers. *Breast Cancer Res.* 2009;11:R15. <https://doi.org/10.1186/bcr2234>.
28. Chen J, Gingold JA, Su X. Immunomodulatory TGF-beta signaling in hepatocellular carcinoma. *Trends Mol Med.* 2019;25:1010–23. <https://doi.org/10.1016/j.molmed.2019.06.007>.
29. Yang Y, et al. The role of TGF-beta signaling pathways in Cancer and its potential as a therapeutic target. *Evid Based Complement Alternat Med.* 2021;2021:6675208. <https://doi.org/10.1155/2021/6675208>.
30. Giannelli G, Mazzocca A, Fransvea E, Lahn M, Antonaci S. Inhibiting TGF-beta signaling in hepatocellular carcinoma. *Biochim Biophys Acta.* 2011;1815:214–23. <https://doi.org/10.1016/j.bbcan.2010.11.004>.
31. Gonzalez-Sanchez E, et al. The TGF-beta pathway: a pharmacological target in hepatocellular carcinoma? *Cancers (Basel).* 2021;13:3248. <https://doi.org/10.3390/cancers13133248>.
32. Chen J, et al. Analysis of genomes and transcriptomes of hepatocellular carcinomas identifies mutations and gene expression changes in the transforming growth factor-beta pathway. *Gastroenterology.* 2018;154:195–210. <https://doi.org/10.1053/j.gastro.2017.09.007>.
33. Khemlina G, Ikeda S, Kurzrock R. The biology of hepatocellular carcinoma: implications for genomic and immune therapies. *Mol Cancer.* 2017;16:149. <https://doi.org/10.1186/s12943-017-0712-x>.
34. Long J, et al. Development and validation of a TP53-associated immune prognostic model for hepatocellular carcinoma. *EBioMedicine.* 2019;42:363–74. <https://doi.org/10.1016/j.ebiom.2019.03.022>.
35. Kavanagh E, Joseph B. The hallmarks of CDKN1C (p57, KIP2) in cancer. *Biochim Biophys Acta.* 2011;1816:50–6. <https://doi.org/10.1016/j.bbcan.2011.03.002>.
36. Guo H, et al. Prognostic significance of co-expression of nm23 and p57 protein in hepatocellular carcinoma. *Hepatol Res.* 2010;40:1107–16. <https://doi.org/10.1111/j.1872-034X.2010.00721.x>.
37. Bai Y, et al. Identification of seven-gene hypoxia signature for predicting overall survival of hepatocellular carcinoma. *Front Genet.* 2021;12:637418. <https://doi.org/10.3389/fgene.2021.637418>.
38. Witt AE, et al. Identification of a cancer stem cell-specific function for the histone deacetylases, HDAC1 and HDAC7, in breast and ovarian cancer. *Oncogene.* 2017;36:1707–20. <https://doi.org/10.1038/ncr.2016.337>.
39. Ler SY, et al. HDAC1 and HDAC2 independently predict mortality in hepatocellular carcinoma by a competing risk regression model in a southeast Asian population. *Oncol Rep.* 2015;34:2238–50. <https://doi.org/10.3892/or.2015.4263>.
40. Vachher M, Arora K, Burman A, Kumar B. NAMPT, GRN, and SERPINE1 signature as predictor of disease progression and survival in gliomas. *J Cell Biochem.* 2020;121:3010–23. <https://doi.org/10.1002/jcb.29560>.
41. Zhu Z, et al. Comprehensive analysis reveals CTHRC1, SERPINE1, VCAN and UPK1B as the novel prognostic markers in gastric cancer. *Transl Cancer Res.* 2020;9:4093–110. <https://doi.org/10.21037/tcr-20-211>.
42. Mazzoccoli G, et al. ARNTL2 and SERPINE1: potential biomarkers for tumor aggressiveness in colorectal cancer. *J Cancer Res Clin Oncol.* 2012;138:501–11. <https://doi.org/10.1007/s00432-011-1126-6>.
43. Jin Y, Liang ZY, Zhou WX, Zhou L. Expression, clinicopathologic and prognostic significance of plasminogen activator inhibitor 1 in hepatocellular carcinoma. *Cancer Biomark.* 2020;27:285–93. <https://doi.org/10.3233/cbm-190560>.
44. Lin Z, Xu Q, Miao D, Yu F. An inflammatory response-related gene signature can impact the immune status and predict the prognosis of hepatocellular carcinoma. *Front Oncol.* 2021;11:644416. <https://doi.org/10.3389/fonc.2021.644416>.
45. Wu G, et al. High levels of BMP2 promote liver Cancer growth via the activation of myeloid-derived suppressor cells. *Front Oncol.* 2020;10:194. <https://doi.org/10.3389/fonc.2020.00194>.
46. Sun Z, et al. Construction of a prognostic model for hepatocellular carcinoma based on Immunoautophagy-related genes and tumor micro-environment. *Int J Gen Med.* 2021;14:5461–73. <https://doi.org/10.2147/ijgm.S325884>.

## Publisher's Note

Springer Nature remains neutral with regard to jurisdictional claims in published maps and institutional affiliations.

Ready to submit your research? Choose BMC and benefit from:

- fast, convenient online submission
- thorough peer review by experienced researchers in your field
- rapid publication on acceptance
- support for research data, including large and complex data types
- gold Open Access which fosters wider collaboration and increased citations
- maximum visibility for your research: over 100M website views per year

At BMC, research is always in progress.

Learn more [biomedcentral.com/submissions](https://biomedcentral.com/submissions)

